Constraints on Standard Model physics from colliders

Kristof Schmieden, on behalf of the ATLAS and CMS collaborations
CERN[1]

E-mail: kristof.schmieden@cern.ch

Abstract. Effective field theories provide an elegant approach to study possible new physics scenarios, by comparing precision measurements with Standard Model predictions. The latest results on multi-boson processes from the ATLAS and CMS collaborations at the LHC, which are sensitive to anomalous gauge couplings and thus can be used to constrain EFT operators, are presented. The consistency of the Standard Model can also be tested by a global electroweak fit to precision observables in the electroweak sector. We present here the precision measurement of the W boson mass as well as the new results on the determination of the electroweak mixing angle and the top quark mass.

1. Introduction

The Standard Model of particle physics (SM) is tremendously successful in understanding the fundamental structure of matter. The precision of theoretical predictions are improving constantly and so are experimental results, confirming the theory predictions to an ever increasing accuracy. Yet despite the huge success of the Standard Model, it is since long known that it is incomplete. Big open questions not answered to date are the nature of neutrinos and dark matter, the origin of the baryon asymmetry in the universe as well as the quantum level description of gravity, to name a few. Without conclusive experimental evidence of new physics in high energy particle processes the question arises at which energies and in which processes physics beyond the Standard Model will appear. These proceedings give an overview of two approaches used by the ATLAS [1] and CMS [2] collaborations at the LHC to find effects from physics beyond the Standard Model in high energy particle collisions.

Section 2 will discuss the usage of an effective field theory (EFT) approach to model non Standard Model contributions to gauge boson couplings. The latest results from the ATLAS and CMS collaborations on the electroweak production of vector boson as well as multi-boson production will be presented, along with the interpretation of the results in terms of limits on contributions of EFT operators. The second approach of finding effects beyond the Standard Model relies on probing the consistency of the Standard Model to the best achievable precision. This is done by performing a global fit of all electroweak parameters of the Standard Model using the most precise experimental measurements, and is detailed in section 3.

2. Constraining Effective Field theory operators using measurements of vector boson production

Effective field theories are expansions in inverse powers of the energy scale of new interactions assuming perturbative coupling coefficients. For a detailed introduction to EFTs see e.g. [3, 4]. Essentially an effective field theory is a systematic Taylor expansion of all occurring variables.

$$f(x) = f(0) + f'(0)x + f''(0)x^2 + ... \tag{1}$$

At low energies (e.g. $\sqrt{s} \approx m_Z$) only simple observables are accessible, like the properties of the Z boson (mass, width, angular distributions) which can be converted into the respective couplings. Contributions from new physics could potentially lead to a rescaling of those couplings. At higher energies $\sqrt{s} \gg m_Z$ however, more and more observables become accessible. Modifications to those are described by higher orders of the Taylor expansion which has to be truncated at some order. The minimal useful order of the Taylor expansion is derived from the most minimal meaningful extension to the Standard Model possible. These are operators of dimension 6, which do not introduce new states and solely lead to modified couplings. In the most recent analyses, however, operators up to dimension 8 are considered. The EFT Lagrangian can then be written as

$$\mathcal{L}_{EFT} = \mathcal{L}_{SM} + \sum_{i=WWW,W,B,\Phi W,\Phi B} \frac{c_i}{\Lambda^2}\mathcal{O}_i + \sum_{j=1,2} \frac{f_{S,j}}{\Lambda^4}\mathcal{O}_{S,j} + \sum_{j=0..9} \frac{f_{T,j}}{\Lambda^4}\mathcal{O}_{T,j} + \sum_{j=0..7} \frac{f_{M,j}}{\Lambda^4}\mathcal{O}_{M,j} \tag{2}$$

where the first term corresponds to dimension 6 operators. Those are sensitive to triple gauge boson couplings (TGC), amongst which only the WWZ and $WW\gamma$ couplings are non-zero at tree level in the SM. The remaining three terms correspond to dimension 8 operators. Those operators contribute to quartic gauge boson couplings (QGC) as well as neutral TGCs. The EFT formalism facilitates a model independent, well defined parametrization of new physics above the mass reach of a given experiment, thus providing an ideal benchmark to assess the impact of SM measurements on the search for new physics phenomena. A historically used alternative to the EFT formalism is referred to as the framework of effective vertex functions [5] in which anomalous coupling vertices are added explicitly to the SM Lagrangian together with complex form factors modifying their contributions. Those form factors are usually labeled h_i^V, $\Delta g, \Delta\kappa, \lambda, \tilde{\kappa}$ and $\tilde{\lambda}$ in literature and some will be presented later on. However, as the estimation of those form factors is model dependent, recent LHC analyses are encouraged to calculate limits on anomalous couplings in term of limits on EFT operators.

Experimentally two approaches are distinguished when studying multi-gauge boson interactions.

(i) Inclusive cross-section measurements of di- and tri-boson final states.

(ii) Measurement of the electroweak production cross-section of single gauge bosons.

Representative Feynman diagrams for both processes are shown in figure 1. Both the ATLAS and CMS collaborations perform a variety of measurements using either approach. A recent, but not exhaustive, summary of measurements of di-boson final states from the CMS collaboration is shown in figure 2(left). A summary of the results on electroweak (EW) production of vector bosons in vector boson fusion (VBF) and vector boson scattering (VBS) analyses is presented in figure 2(right). In the following a selection of analyses will be presented which is by no means exhaustive. Usually corresponding analyses are performed by both the ATLAS and CMS collaborations. For a complete list of measurements performed please refer to [6] and [7], respectively. Overall no significant deviations from the SM predictions have been observed so far.

Selected results from studies of inclusive multi-boson production are presented in section 2.1, followed by selected results of measurements studying the electroweak production of single vector bosons in section 2.2.

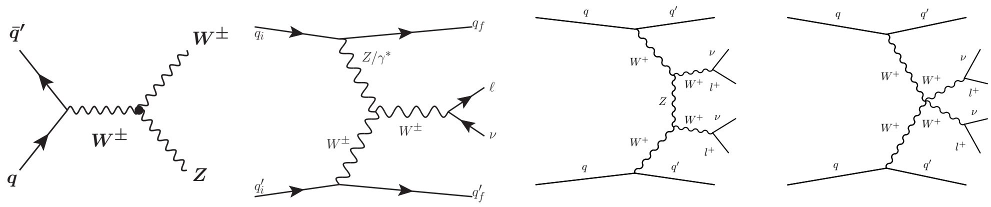

Figure 1. Feynman diagrams showing from left to right: the tree-level process for WZ production, electroweak production of a W boson, WW boson pair production involving TGCs and QGC.

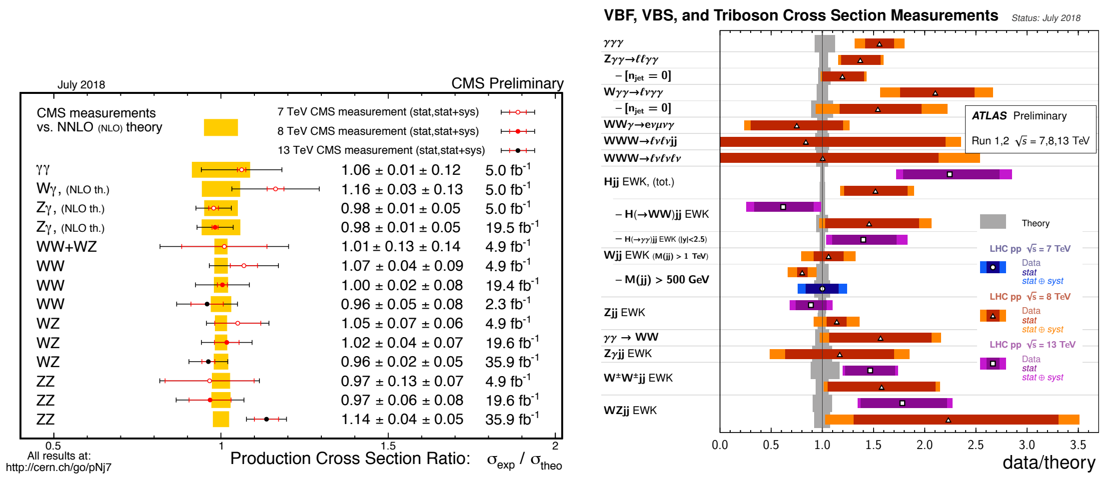

Figure 2. Overviews of di-boson production cross-section measurements from the CMS collaboration (left) [7] as well as VBF, VBS and tri-boson production cross-section measurements from the ATLAS collaboration (right) [6].

2.1. Inclusive production of multiple gauge bosons

The measurement of the differential production cross-section of a Z boson together with a photon is performed by ATLAS using $36\,\mathrm{fb}^{-1}$ of 13 TeV pp collisions data [8]. The invisible Z boson decay into neutrinos is utilized in this analysis. Studying the Z boson decay into neutrinos has several advantages over processes where the Z boson decays into hadrons or charged leptons. The hadronic decay channel is contaminated with a large multi-jet background. A larger Z boson branching ratio into neutrinos relative to that into charged leptons provides an opportunity to study this process for larger photon transverse energies (E_{T}^{γ}), where the sensitivity bosonic couplings is higher. In addition, the neutrino channel is sensitive to anomalous neutrino dipole moments, although a larger integrated luminosity than that available to this study would be required to significantly improve upon the LEP results [9]. Events featuring photons with $E_{\mathrm{T}}^{\gamma} > 600\,\mathrm{GeV}$ are used to set limits on anomalous triple gauge couplings (aTGC). Uncertainties on aTGC limits estimated from the $Z\gamma$ final state were reduced by a factor 4 to 7 within last two years, profiting from the increased LHC beam energy and a larger data set. This is visible in figure 3, where the parameters $h_{3,4}^{\gamma}$, calculated using the framework of effective vertex functions, are compared between the ATLAS measurement performed in 2016 using $20.3\mathrm{fb}^{-1}$ of 8 TeV data [10] and the one from 2018 presented here.

The only TGC between W and Z bosons allowed in the SM is the WWZ coupling. This can be studied using WZ final states to search for any additional anomalous WWZ couplings. Such

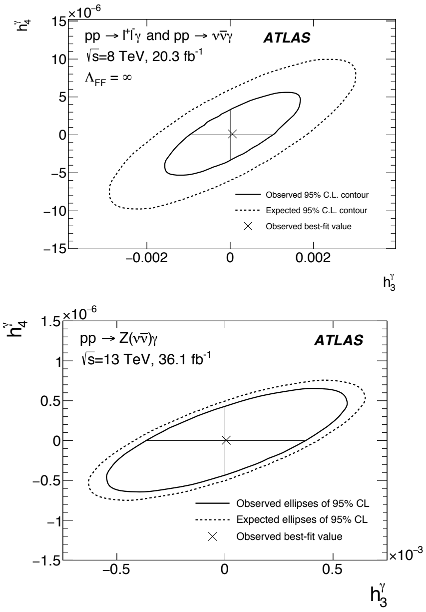

Figure 3. 95% C.L. limits on h_3 and h_4, extracted from the study of $Z(\bar{\nu}\nu)\gamma$ events published in 2016 [10] (top) and 2018 [8] (bottom).

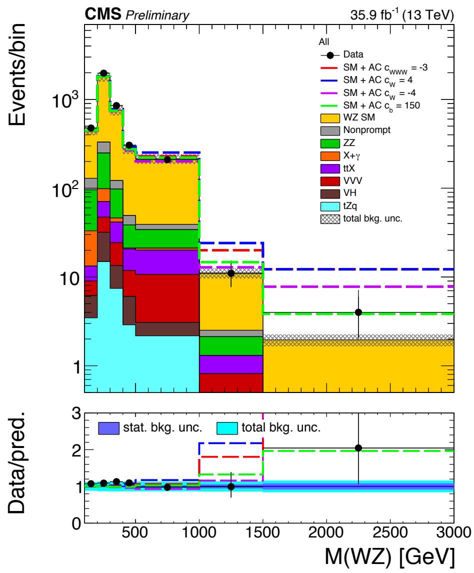

Figure 4. Measured invariant mass distribution of WZ boson pairs (black markers) compared to the SM expectation (shaded histograms) and predictions with modified coupling parameters (dashed lines)[12].

analyses have been performed by both the ATLAS [11] and CMS [12] collaborations yielding similar results. Anomalous couplings changing the WWZ vertex would result in an altered invariant mass distribution of the selected WZ events. Measurement and predictions for various modified coupling scenarios are shown in figure 4. As no deviation from the SM expectation is observed limits are set on the EFT parameters contributing to anomalous WWZ couplings and shown in table 1 together with results from various other analyses.

Finally, the three-boson final state is sensitive to QGCs and a total of 16 dimension 8 EFT operators. Events containing $WW\gamma$ or $WZ\gamma$ boson triplets have been studied by the ATLAS collaboration [17]. Two final state signatures are considered: $e\nu\mu\nu\gamma$ which is enriching $WW\gamma$ events and $e\nu jj\gamma$ enriching $WZ\gamma$ events. One of the variables that is most sensitive to the EFT operators is the photon transverse energy, which is shown for the $e\nu jj\gamma$ selection in figure 5 together with the limits set on all accessible dimension 8 operators.

2.2. Electroweak production of vector bosons

The fusion of vector bosons is a particularly important process for measuring particle properties, such as the couplings of the Higgs boson, as well as for searching for new particles beyond the SM. It is a sensitive probe of anomalous couplings of vector bosons. Several analyses from the ATLAS and CMS collaborations study EW production of single vector bosons as well as di-vector boson production. In pp collisions, a characteristic signature of these processes is the production of two high-momentum jets of hadrons at small angles with respect to the incoming proton beams.

Several topologies are studied using dedicated analyses: single W or Z boson production, same sign $W^{\pm}$ pair production and $W^{\pm}Z$ pair production. EW production of single vector bosons is sensitive to the WWZ TGC, as can be seen from figure 1. A variety of analyses have been performed using W or Z bosons in the final state [15, 16, 18–22]. The results are

Table 1. Overview of expected and observed 1-D confidence intervals at 95% confidence level for various analyses presented throughout section 2.

Analysis	Parameter	(expected) [TeV^{-2}]	(observed) [TeV^{-2}]
WZ [12]	c_w/Λ^2	[-3.3, 2.0]	[-4.1, 1.1]
WV [13]	c_w/Λ^2	[-6.0, 6.7]	[-5.1, 5.8]
WV [14]	c_w/Λ^2	-	[-2.0, 5.7]
Zjj [15]	c_w/Λ^2	[-12.6, 14.7]	[-8.4, 10.1]
Wjj [16]	c_w/Λ^2	[-39, 37]	[-33, 30]
WZ [12]	c_{www}/Λ^2	[-1.8, 1.9]	[-2.0, 2.1]
WV [13]	c_{www}/Λ^2	[-3.6, 3.6]	[-3.1, 3.1]
WV [14]	c_{www}/Λ^2	-	[-2.7, 2.7]
Zjj [15]	c_{www}/Λ^2	[-3.7, 3.6]	[-2.6, 2.6]
Wjj [16]	c_{www}/Λ^2	[-16, 13]	[-13, 9]
WZ [12]	c_B/Λ^2	[-130, 170]	[-100, 160]
WV [13]	c_B/Λ^2	[-22, 23]	[-19, 20]
WV [14]	c_B/Λ^2	-	[-14, 17]
Wjj [16]	c_B/Λ^2	[-200, 190]	[-170, 160]
Wjj [16]	$c_{\tilde{W}/\Lambda^2}$	[-720, 720]	[-580, 580]
Wjj [16]	$c_{\tilde{W}WW/\Lambda^2}$	[-14, 14]	[-11, 11]

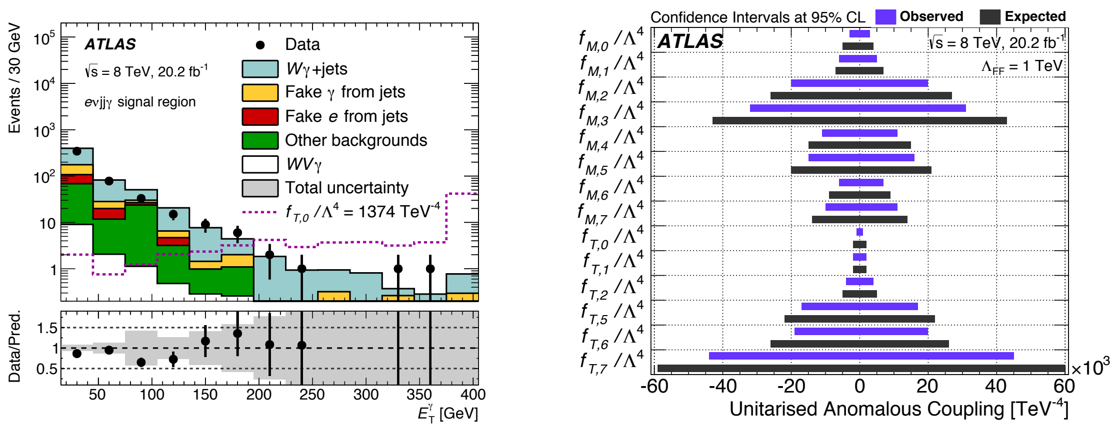

Figure 5. The left plot shows the $e\nu jj\gamma$ signal region of the tri-boson analysis [17], which is sensitive to quartic gauge couplings. Extracted limits on dimension 8 EFT operators are shown in the right plot.

summarized in figure 6. Those are turned into limits on EFT parameters or limits on anomalous coupling form factors in the framework of effective vertex functions. The most stringent limits are derived from the Zjj final state, whereas more operators have been studied in the Wjj final state. A summary of the limits on the EFT operators from several analyses is given in table 1.

The EW production of two vector bosons has been studied in several recent analyses as well [23, 24]. Of particular interest is the EW production of two same charge W bosons, i.e. the scattering process of two W bosons, to which tripple and quartic gauge couplings contribute as well as Higgs boson exchange. The latter leads to large cancelations between the Feynman diagrams involved, restoring the unitarity of the SM. Hence this process is a fundamental probe of the electroweak symmetry breaking and was first observed by the CMS collaboration in 2017

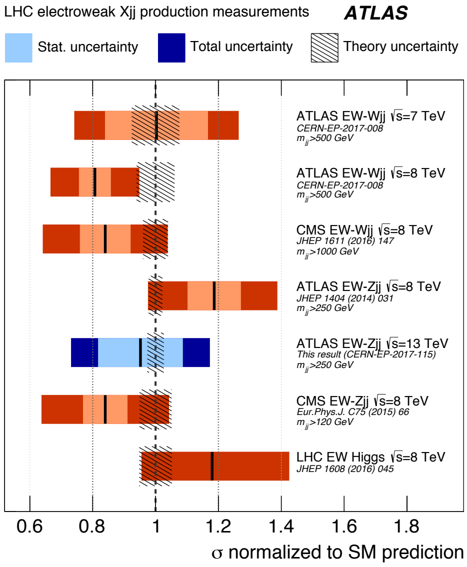

Figure 6. Overview of recent results on cross-section measurements for electroweak Vjj production from the ATLAS and CMS collaborations [6].

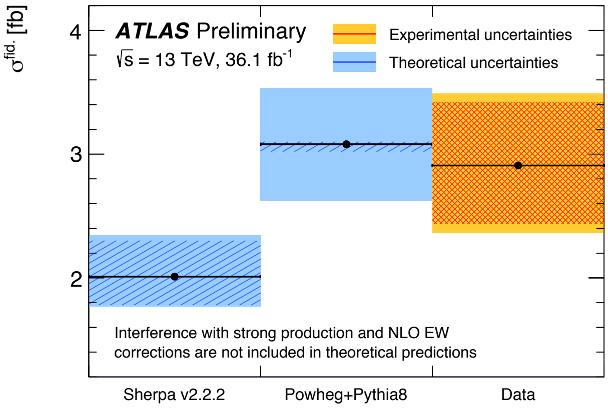

Figure 7. Predicted WW boson pair production cross-sections by Sherpa and Powheg+Pythia (blue) in comparison to the measurement (orange) [23].

[25] with a significance of $5.5\,\sigma$ ($5.7\,\sigma$ expected), and recently by the ATLAS collaboration with a significance of $6.9\,\sigma$ ($4.6\,\sigma$ expected) [23]. The measurements have been used to set limits on various dimension 8 EFT operators. The same sign WW production process is the only di-boson process to date for which EW and QCD NLO corrections have been computed [26]. Including NLO EW correction shifts the predicted cross-section by -15% in the fiducial region and significantly reduces the uncertainties from around 10% to 2%. Significant differences in the cross-section prediction by the Sherpa [27] and Powheg [28] event generators have been observed in [23] which is shown in figure 7.

The EW production of a W boson together with a Z boson is another key probe of the gauge symmetry in the electroweak sector of the SM as it is directly sensitive to the vector boson self-coupling. This process has recently been observed by the ATLAS collaboration for the first time [29] with a significance of $5.6\,\sigma$ ($3.3\,\sigma$ expected). The measured fiducial cross-section of the EW production of the WZ boson pair is measured to be

$$\sigma_{meas.}^{\text{fid.,EW}} = 0.57^{+0.14}_{-0.13}(\text{stat})^{+0.05}_{-0.04}(\text{syst})^{+0.04}_{-0.03}(\text{th})\text{fb}.$$

Currently only LO EW predictions are available for this process. Sherpa v2.2.2 predicts a cross-section of $\sigma_{Sherpa}^{\text{fid.,EW}} = 0.32 \pm 0.03\,\text{fb}$, significantly below the measurement. Triple and quartic gauge couplings contribute to the WZ pair production and hence this process can be used to set limits on several EFT parameters. This was done in a recent analysis by CMS [24] which provided limits on several dimension 8 operators. In addition the analysis exhibits sensitivity to the decay of a hypothetical charged Higgs boson into a WZ pair. As no evidence for such a process has been observed, limits were set accordingly.

All of the analyses involving multi-boson final states are limited by the size of the available datasets. Hence significant improvements can be expected with the analysis of the full LHC run-2 data set and even more so using the future data from LHC run-3 and beyond. An estimate of the evolutions of the cross-section uncertainty for the vector boson scattering processes has been presented in [30]. Analyses discussed in these proceedings use an integrated luminosity of $36\,\mathrm{fb}^{-1}$ at most. A factor 3 improvement on the uncertainty can be expected until the end of run-3, assuming an integrated luminosity of $300\,\mathrm{fb}^{-1}$. At the end of the HL-LHC data taking a reduction of the uncertainty by a factor of ≈ 8 with respect to the current analyses is expected.

3. Global electroweak fit

Simultaneous fitting of all SM electroweak parameters to theory calculations is a unique way of combining experimental electroweak precision observables with the most accurate theoretical calculations available in a global way. This has proven very successful in the past in predicting e.g. the masses of the top quark and the Higgs boson. It is also a comprehensive test of the consistency of the SM as illustrated in figure 8(top), which was released with the latest update of the results from the GFitter group [31]. Recent theory calculations used in the global fit include full two loop EW terms (NNLO) and even partial 3 and 4 loop terms. The latest updates of the experimental inputs include an updated measurement of the W boson mass, the top quark mass as well as the weak mixing angle and the Higgs mass.

The results of the global fit impressively confirm the consistency of the SM within the current experimental uncertainty. The calculated $\chi^2_{min}/\mathrm{d.o.f.} = 18.6/15$ yields a probability of 23%. The largest potential for improvement lies in the W boson mass measurement, where the experimental uncertainty (13 MeV) and the uncertainty from the fit (7 MeV) have the same order of magnitude and the global fit is pulled by the measurement. Hence this observable should be assigned the highest priority for experimental improvements. The only, long lasting, tension visible in figure 8(left) is found between the asymmetry measurements $A^{0,b}_{FB}$ and $A_l(SLD)$ from LEP and SLD. A new generation of analyses at the LHC measuring the leptonic electroweak mixing angle may eventually resolve the tension.

Measurements for three input parameters to the global electroweak fit will be presented, namely the measurements of m_W, the weak mixing angle and the top quark mass.

3.1. Measurement of the W boson mass

When studying inclusive W boson decays two variables are sensitive to its mass. The transverse momentum distribution of the decay lepton p_T^l exhibits a Jacobean peak at $m_W/2$ at tree level. The distribution of the transverse mass, which is defined as $m_T = \sqrt{2p_\mathrm{T}^l p_\mathrm{T}^{miss}(1-\cos\Delta\phi)}$, has an endpoint corresponding to the mass of the W boson. Here p_T^{miss} is the missing transverse momentum of the event and $\Delta\phi$ is the difference in azimuth between the decay lepton and the missing transverse energy, which is associated to the neutrino from the W boson decay. Various effects modify the reconstructed p_T^l and m_T distributions, the most prominent ones being QED initial state radiation, the unknown transverse momentum of the W boson due to QCD effects as well as the detector response. The latest measurement of the W mass was released by the ATLAS collaboration in 2018 [32]. In this analysis both sensitive distributions were fitted independently to templates generated by simulation in 14 different event categories, separated in bins of η^l, by the W boson charge as well as electron and muon final states. Both, p_T^l and m_T, exhibit different sensitivity to additional effects. The m_T distribution is sensitive to the hadronic recoil resolution, but exhibits only a low sensitivity to the transverse momentum of the W boson. In contrast, the p_T^l distribution is directly sensitive to p_T^W but less dependent on the hadronic recoil measurement. The combination of all measurement channels yields a W boson mass of

$$m_W = 80370 \pm 7(\mathrm{stat.}) \pm 11(\mathrm{exp.syst.}) \pm 14(\mathrm{mod.syst.})\,\mathrm{MeV} = 80370 \pm 19\,\mathrm{MeV}\,. \tag{3}$$

Results for individual W boson charges are shown along results from other experiments in Figure 9 (left). The largest uncertainty arises from the modeling of the W boson transverse momentum distribution, which is theoretically very difficult to describe. Hence the more precise

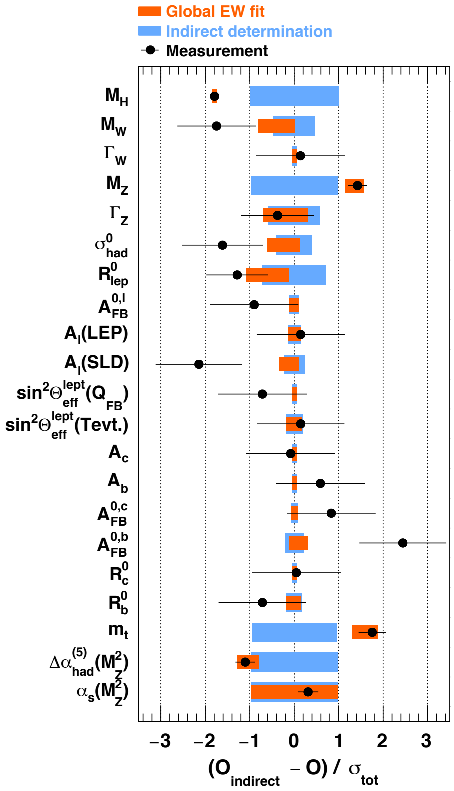

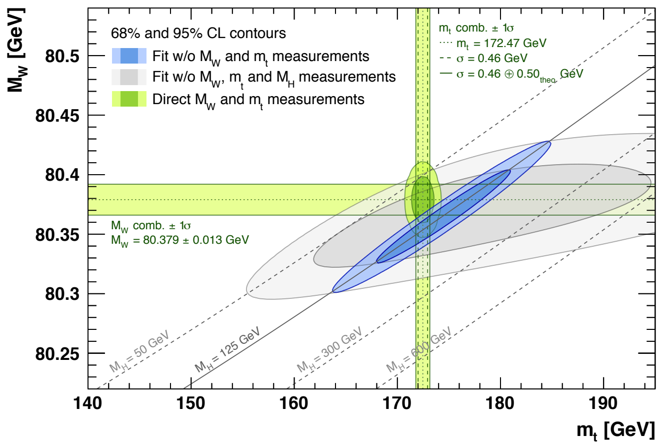

Figure 8. GFitter results [31]. (Left): comparison of input measurements to fit results and indirect determinations in units of the total uncertainties. The latter corresponds to a fit without using the constraint from the corresponding input measurement. (Top): Contours at 68% and 95% CL obtained from scans of m_W versus m_t for the global fit including (blue) and excluding (grey) the m_H measurement. Direct measurements and their $1\,\sigma$ errors are shown as green bands (ellipses show $1\,\sigma$ and $2\,\sigma$ errors).

measurement of the transverse momentum of the Z boson is transformed into the expected p_{T}^{W} distribution using predictions of the ratio $\sigma_Z/\sigma_W(p_{\mathrm{T}})$. Interestingly, different predictions of this ratio disagree significantly, in particular for low values of $p_{\mathrm{T}}^{W,Z}$, as is presented in [33]. A measurement of p_{T}^{W} in bins of 5 GeV with an accuracy of 1% is needed to significantly reduce this uncertainty. This could be achieved utilizing the data recorded under low pileup conditions by the ATLAS and CMS experiments, which amounts to $\approx 500\,\mathrm{pb}^{-1}$. Expected uncertainties for various PDFs in conjunction with the analysis of $200\,\mathrm{pb}^{-1}(1\,\mathrm{fb}^{-1})$ of low pileup data are presented in figure 9 (right), where a significant reduction of uncertainties is expected using a small amount of low pileup data. Other major contributions to the uncertainty on m_W arise from the uncertainties on the lepton reconstruction efficiency and calibration as well as uncertainties due to PDFs. Results from the most precise measurement of inclusive W, Z production performed using the 7 TeV LHC dataset were used to determine the PDF set that best describes the data used for the measurement of m_W to be the CT10 PDF. The uncertainty due to PDFs were assesed using this and comparisons to two additional PDF sets.

3.2. Measurement of the leptonic weak mixing angle

The full event information of the inclusive Z boson production and subsequent decay into lepton pairs can be described by the 5-dimensional differential cross-section which in turn can be

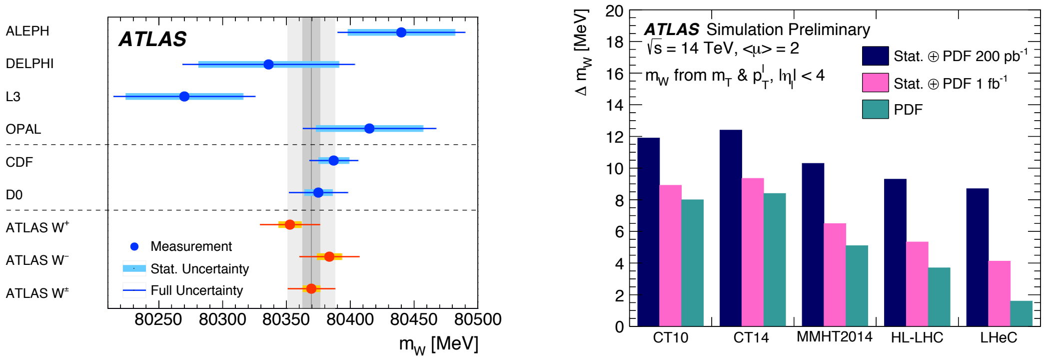

Figure 9. Results from the ATLAS m_W measurements are shown along with previous results in the left figure [32]. Estimates of the expected uncertainty on m_W are shown for various PDF sets assuming $200\,\mathrm{pb}^{-1}(1\,\mathrm{fb}^{-1})$ of low pileup data in the right figure [34].

decomposed into 1+8 othortogonal polynomials

$$\frac{d\sigma}{dp_{\mathrm{T}}^{ll}dy^{ll}dm^{ll}d\cos\theta d\phi} = \frac{3}{16\pi}\frac{d\sigma^{U+L}}{dp_{\mathrm{T}}^{ll}dy^{ll}dm^{ll}} \cdot$$

$$\Big\{\tfrac{1}{2}A_0\left(1-3\cos^2\theta\right) + A_1\sin 2\theta\cos\phi + \tfrac{1}{2}A_2\sin^2\theta\cos 2\phi + A_3\sin\theta\cos\phi + A_4\cos\theta$$

$$+A_5\sin\theta\sin 2\phi + A_6\sin 2\theta\sin\phi + A_7\sin\theta\sin\phi\Big\} \qquad (4)$$

with θ, ϕ being the polar and azimuth angles of the final state lepton. The coefficients A_i are themselves functions of p_{T}^{ll}, y^{ll} and m^{ll} and have been measured by ATLAS [35]. A_4 is directly related to the forward-backward asymmetry in the full phase space via the relation $A_{FB} = A_4 \cdot 3/8$, where $A_{FB} = (\sigma_{\cos\theta>0} - \sigma_{\cos\theta<0})/\sigma$. A_4 and hence A_{FB} are sensitive to the effective weak mixing angle $\sin^2\theta_{\mathrm{W}}^{eff}$. The coefficient A_3 also exhibits some sensitivity to $\sin^2\theta_{\mathrm{W}}^{\mathrm{eff}}$ but is not used in the presented analyses.

The CMS collaboration measured the double differential forward-backward asymmetry $A_{FB}(m^{ll}, y^{ll})$ [36] independently in electron and muon final states. The double differential measurement allows to simultaneously constrain the PDF used in the analysis and extract $\sin^2\theta_{\mathrm{W}}^{\mathrm{eff}}$, which significantly reduces the uncertainty due to the PDFs. The analysis uses templates generated for various values of $\sin^2\theta_{\mathrm{W}}^{\mathrm{eff}}$ using Powheg in conjunction with the NNPDF3.0 PDF set. Those templates are fitted to measured distributions yielding the value of $\sin^2\theta_{\mathrm{W}}^{\mathrm{eff}}$ found in data. One hundred PDF replicas were used to generate weights according to their agreement with the measured A_{FB} distribution. Using the constraints on the PDF reduces the uncertainty from the PDF from $57{\cdot}10^{-5}$ to $31{\cdot}10^{-5}$. The largest systematic uncertainty arises from the limited size of the simulated event sample, contributing an uncertainty of $15(33){\cdot}10^{-5}$ in the muon (electron) channels, respectively. The largest theory uncertainties arise from variations of the renormalisation and factorization scales in the event simulation. The final result for the effective leptonic weak mixing angle after combining the electron and muon channels is shown in table 2, together with results from ATLAS and the Tevatron experiments.

ATLAS uses $A_4(p_{\mathrm{T}}^{ll}, y^{ll}, m^{ll})$ to extract $\sin^2\theta_{\mathrm{W}}^{\mathrm{eff}}$. A_4 was measured in three independent channels using muons in the final state, electrons with both electrons being within $|\eta| < 2.4$ and the so called central-forward channel where one electron lies within $|\eta| < 2.4$ and one electron within $2.5 < |\eta| < 3.2$. A linear parametrization of A_4 in terms of $\sin^2\theta_{\mathrm{W}}^{\mathrm{eff}}$ was derived using the improved Born approximation (IBA) including NLO EW effects. The impact of

Table 2. Recent measurements of $\sin^2\theta^l_{\text{eff}}$.

Experiment	$\sin^2\theta^l_{\text{eff}}$	stat. $[10^{-5}]$	syst. $[10^{-5}]$	theo. $[10^{-5}]$	PDF $[10^{-5}]$
CMS [36]:	0.23101 ± 0.0053	36	18	16	31
ATLAS [37]:	0.23140 ± 0.0037	21	16	-	24
D0 + CDF [38]:	0.23148 ± 0.0033	27	05	-	18

NLO EW contributions on the analysis was studied in great detail as those could potentially break the factorization of the cross-section into the polynomials shown in equation 4. For this purpose the results from calculations using the IBA where transferred to the EW LO Powheg simulation by means of form factors. Though the factorization is shown to be preserved, the impact on the extraction of $\sin^2\theta^{\text{eff}}_{\text{W}}$ amounts to about the same size as the uncertainty from the A_4 measurement. Hence NLO EW effects are included throughout the analysis. Details are presented in Ref. [37]. The Tevatron collaborations CDF and D0 recently released an updated result of a similar measurement, utilizing the single differential measurement of $A_{FB}(m^{ll})$ as sensitive variable [38]. The result is presented in table 2. All results are in agreement with each other, and are also consistent with the combined result from the LEP and SLD experiments.

3.3. Measurements of the top mass

The measured mass of the top quark m_t is another important input to the global electroweak fit. Two distinct methods are used to measure the top mass. In the direct measurement the full event kinematic is reconstructed and variables sensitive to m_t are compared to simulated templates. Essentially this method measures a parameter in the simulation, often called $m^{\text{MC}}_{\text{top}}$. The difficulty in this approach lies in the conversion of the measured parameter of the simulation to the theoretically well defined pole mass of the top quark and this leads to ambiguities. On the other hand the indirect measurement of m_t exploits the dependence of the $t\bar{t}$ production cross-section on the top pole mass. Essentially the mass measurement is turned into a cross-section measurement and $\sigma_{t\bar{t}}$ is compared to theory calculation in order to extract m_t. This allows to unambiguously measure the top pole mass within the renormalisation scheme adopted for the cross-section measurement. However, this approach is largely sensitive to the PDF used in the cross-section predictions which in turn leads to significant uncertainties.

The latest top mass measurement from the ATLAS collaboration [39] uses the direct measurement approach yielding $m_t = 172.08 \pm 0.39(stat.) \pm 0.82(syst.)$ GeV. The latest result from the CMS collaboration [40] uses both, the indirect and direct mass measurements, yielding results of $m^{\text{MC}}_t = 172.33 \pm 0.14(stat.)^{+0.66}_{-0.72}(syst.)$ GeV and $m^{\text{pole}}_{t,\text{NNPDF3.0}} = 172.4 \pm 1.6(\text{fit} + \text{PDF} + \alpha_s)^{+1.3}_{-2.0}(scale)$ GeV. A large variety of top mass measurements have been released by the ATLAS and CMS collaborations, utilizing various final states and measurement methods. An overview is given in figure 10 (left). The latest compilation of all available top pole mass results was released in March 2018 [41] and is presented in figure 10 (right).

4. Summary

Over the past two years impressive progress has been made studying the SM gauge couplings as well as the EW parameters at the LHC experiments. New multi-boson processes became experimentally accessible, and limits on anomalous gauge couplings are narrowed down bit by bit. The first measurement of the W boson mass at the LHC was released as well as precision measurements on EW observables. No evidence of physics beyond the SM was observed and all results confirm the consistency of the SM to unprecedented accuracy. Many analyses, in

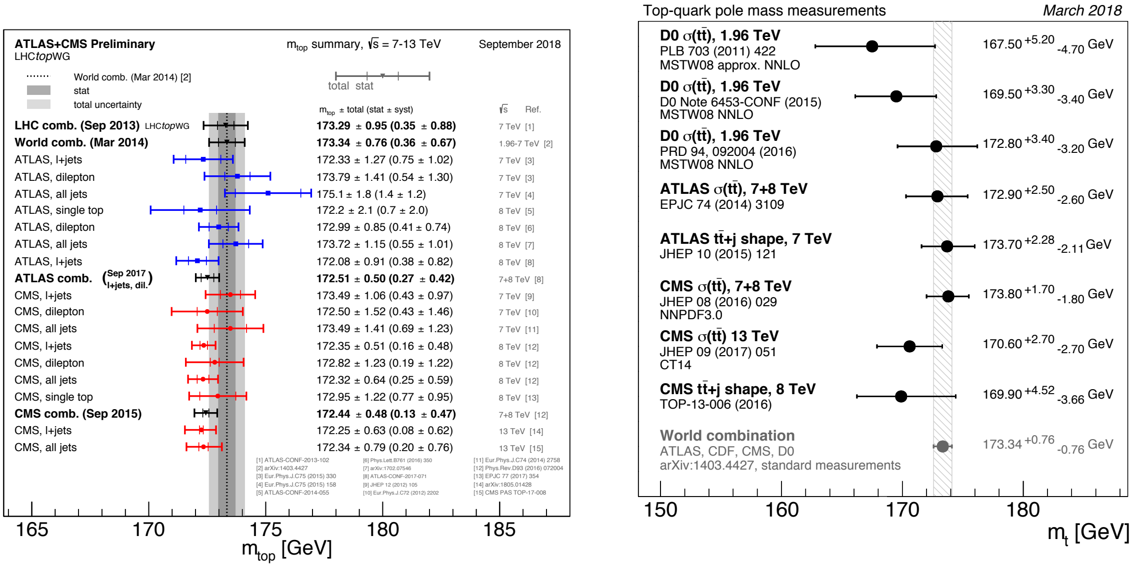

Figure 10. An overview of top quark mass measurement results performed at ATLAS and CMS is given in the left figure [42]. Various top quark pole mass measurements are compared to the world combination in the right figure.

particular those targeting multi-gauge boson final states, are limited by the available statistics. Hence significant improvements are expected from results using the full dataset recorded during the LHC run-2, and even more so once the LHC run-3 data will be available.

References

[1] ATLAS Collaboration. "The ATLAS Experiment at the CERN Large Hadron Collider". In: *JINST* 3 (2008), S08003.

[2] CMS Collaboration. "The CMS experiment at the CERN LHC". In: *JINST* 3 (2008), S08004.

[3] C. Degrande et al. "Effective Field Theory: A Modern Approach to Anomalous Couplings". In: *Annals Phys.* 335 (2013), pp. 21–32. arXiv: `1205.4231 [hep-ph]`.

[4] C. Degrande. "A basis of dimension-eight operators for anomalous neutral triple gauge boson interactions". In: *JHEP* 02 (2014), p. 101. arXiv: `1308.6323 [hep-ph]`.

[5] U. Baur and E. L. Berger. "Probing the weak-boson sector in $Z\gamma$ production at hadron colliders". In: *Phys. Rev. D* 47 (11 June 1993), pp. 4889–4904.

[6] ATLAS Collaboration. *ATLAS public standard model results*. 2019. URL: `https://twiki.cern.ch/twiki/bin/view/AtlasPublic/StandardModelPublicResults` (visited on 03/03/2019).

[7] CMS Collaboration. *CMS public standard model results*. 2019. URL: `http://cms-results.web.cern.ch/cms-results/public-results/publications/SMP/index.html` (visited on 03/03/2019).

[8] ATLAS Collaboration. "Measurement of the $Z\gamma \to \nu\bar{\nu}\gamma$ production cross section in pp collisions at $\sqrt{s} = 13$ TeV with the ATLAS detector and limits on anomalous triple gauge-boson couplings". In: *JHEP* (2018). arXiv: `1810.04995 [hep-ex]`.

[9] A. Gutierrez-Rodriguez et al. *Studies on the anomalous magnetic and electric dipole moments of the tau-neutrino in pp collisions at the LHC*. arXiv: `1712.02439 [hep-ph]`.

[10] ATLAS Collaboration. “Measurements of $Z\gamma$ and $Z\gamma\gamma$ production in pp collisions at $\sqrt{s} = 8$ TeV with the ATLAS detector”. In: *Phys. Rev. D* 93 (2016), p. 112002. arXiv: `1604.05232 [hep-ex]`.

[11] ATLAS Collaboration. *Measurement of $W^{\pm}Z$ boson pair-production in pp collisions at $\sqrt{s} = 13$ TeV with the ATLAS Detector and confidence intervals for anomalous triple gauge boson couplings.* ATLAS-CONF-2016-043. 2016. URL: `https://cds.cern.ch/record/2206093`.

[12] CMS Collaboration. “Measurements of the pp→WZ inclusive and differential production cross section and constraints on charged anomalous triple gauge couplings at $\sqrt{s} = 13$ TeV”. In: *submited to JHEP* (2019). arXiv: `1901.03428 [hep-ex]`.

[13] ATLAS Collaboration. “Measurement of $WW/WZ \to \ell\nu qq'$ production with the hadronically decaying boson reconstructed as one or two jets in pp collisions at $\sqrt{s} = 8$ TeV with ATLAS, and constraints on anomalous gauge couplings”. In: *Eur. Phys. J. C* 77 (2017), p. 563. arXiv: `1706.01702 [hep-ex]`.

[14] CMS Collaboration. “Search for anomalous couplings in boosted $WW/WZ \to \ell\nu q\bar{q}$ production in proton–proton collisions at $\sqrt{s} = 8$ TeV”. In: *Phys. Lett. B* 772 (2017), p. 21. arXiv: `1703.06095 [hep-ex]`.

[15] CMS Collaboration. “Electroweak production of two jets in association with a Z boson in proton–proton collisions at $\sqrt{s} = 13$ TeV”. In: *Eur. Phys. J. C* 78 (2018), p. 589. arXiv: `1712.09814 [hep-ex]`.

[16] ATLAS Collaboration. “Measurements of electroweak Wjj production and constraints on anomalous gauge couplings with the ATLAS detector”. In: *Eur. Phys. J. C* 77 (2017), p. 474. arXiv: `1703.04362 [hep-ex]`.

[17] ATLAS Collaboration. “Study of $WW\gamma$ and $WZ\gamma$ production in pp collisions at $\sqrt{s} = 8$ TeV and search for anomalous quartic gauge couplings with the ATLAS experiment”. In: *Eur. Phys. J. C* 77 (2017), p. 646. arXiv: `1707.05597 [hep-ex]`.

[18] ATLAS Collaboration. “Observation of electroweak $W^{\pm}Z$ boson pair production in association with two jets in pp collisions at $\sqrt{s} = 13$ TeV with the ATLAS detector”. In: *Phys. Lett.* (2018). arXiv: `1812.09740 [hep-ex]`.

[19] ATLAS Collaboration. “Measurement of the cross-section for electroweak production of dijets in association with a Z boson in pp collisions at $\sqrt{s} = 13$ TeV with the ATLAS detector”. In: *Phys. Lett. B* 775 (2017), p. 206. arXiv: `1709.10264 [hep-ex]`.

[20] ATLAS Collaboration. “Studies of $Z\gamma$ production in association with a high-mass dijet system in pp collisions at $\sqrt{s} = 8$ TeV with the ATLAS detector”. In: *JHEP* 07 (2017), p. 107. arXiv: `1705.01966 [hep-ex]`.

[21] CMS Collaboration. “Measurement of the cross section for electroweak production of $Z\gamma$ in association with two jets and constraints on anomalous quartic gauge couplings in proton–proton collisions at $\sqrt{s} = 8$ TeV”. In: *Phys. Lett. B* 770 (2017), p. 380. arXiv: `1702.03025 [hep-ex]`.

[22] CMS Collaboration. “Measurement of electroweak production of a W boson and two forward jets in proton–proton collisions at $\sqrt{s} = 8$ TeV”. In: *JHEP* 11 (2016), p. 147. arXiv: `1607.06975 [hep-ex]`.

[23] ATLAS Collaboration. *Observation of electroweak production of a same-sign W boson pair in association with two jets in pp collisions at $\sqrt{s} = 13$ TeV with the ATLAS detector.* ATLAS-CONF-2018-030. 2018. URL: `https://cds.cern.ch/record/2629411`.

[24] CMS Collaboration. *Measurement of electroweak WZ boson production and search for new physics in WZ + two jets events in pp collisions at $\sqrt{s} = 13$ TeV.* 2019. arXiv: `1901.04060 [hep-ex]`.

[25] CMS Collaboration. "Observation of Electroweak Production of Same-Sign W Boson Pairs in the Two Jet and Two Same-Sign Lepton Final State in Proton–Proton Collisions at 13 TeV". In: *Phys. Rev. Lett.* 120 (2018), p. 081801. arXiv: `1709.05822 [hep-ex]`.

[26] B. Biedermann, A. Denner, and M. Pellen. "Large Electroweak Corrections to Vector-Boson Scattering at the Large Hadron Collider". In: *Physical Review Letters* 118 (Nov. 2016).

[27] S. Schumann and F. Krauss. "A Parton shower algorithm based on Catani-Seymour dipole factorisation". In: *JHEP* 03 (2008), p. 038. arXiv: `0709.1027 [hep-ph]`.

[28] S. Frixione, P. Nason, and C. Oleari. "Matching NLO QCD computations with Parton Shower simulations: the POWHEG method". In: *JHEP* 11 (2007), p. 070. arXiv: `0709.2092 [hep-ph]`.

[29] ATLAS Collaboration. *Observation of electroweak $W^{\pm}Z$ boson pair production in association with two jets in pp collisions at $\sqrt{s} = 13$ TeV with the ATLAS detector.* ATLAS-CONF-2018-033. 2018. URL: `https://cds.cern.ch/record/2630183`.

[30] ATLAS Collaboration. *HL-LHC prospects for diboson resonance searches and electroweak vector boson scattering in the $WW/WZ \to \ell\nu qq$ final state.* ATL-PHYS-PUB-2018-022. 2018. URL: `https://cds.cern.ch/record/2645269`.

[31] J. Haller et al. "Update of the global electroweak fit and constraints on two-Higgs-doublet models". In: *Eur. Phys. J.* C78.8 (2018), p. 675. arXiv: `1803.01853 [hep-ph]`.

[32] ATLAS Collaboration. "Measurement of the W-boson mass in pp collisions at $\sqrt{s} = 7$ TeV with the ATLAS detector". In: *Eur. Phys. J. C* 78 (2018), p. 110. arXiv: `1701.07240 [hep-ex]`.

[33] ATLAS Collaboration. *Prospects for the measurement of the W-boson transverse momentum with a low pileup data sample at $\sqrt{s} = 13$ TeV with the ATLAS detector.* ATL-PHYS-PUB-2017-021. 2017. URL: `https://cds.cern.ch/record/2298152`.

[34] ATLAS Collaboration. *Prospects for the measurement of the W-boson mass at the HL- and HE-LHC.* ATL-PHYS-PUB-2018-026. 2018. URL: `https://cds.cern.ch/record/2645431`.

[35] ATLAS Collaboration. "Measurement of the angular coefficients in Z-boson events using electron and muon pairs from data taken at $\sqrt{s} = 8$ TeV with the ATLAS detector". In: *JHEP* 08 (2016), p. 159. arXiv: `1606.00689 [hep-ex]`.

[36] CMS Collaboration. "Measurement of the weak mixing angle using the forward-backward asymmetry of Drell–Yan events in pp collisions at 8 TeV ". In: *Eur. Phys. J. C* 78 (2018), p. 701. arXiv: `1806.00863 [hep-ex]`.

[37] ATLAS Collaboration. *Measurement of the effective leptonic weak mixing angle using electron and muon pairs from Z-boson decay in the ATLAS experiment at $\sqrt{s} = 8$ TeV.* ATLAS-CONF-2018-037. 2018. URL: `https://cds.cern.ch/record/2630340`.

[38] T. A. Aaltonen et al. "Tevatron Run II combination of the effective leptonic electroweak mixing angle". In: *Phys. Rev.* D97.11 (2018), p. 112007. arXiv: `1801.06283 [hep-ex]`.

[39] ATLAS Collaboration. "Measurement of the top quark mass in the $t\bar{t} \to$ lepton+jets channel from $\sqrt{s} = 8$ TeV ATLAS data and combination with previous results". In: *Eur. Phys. J.* (2018). arXiv: `1810.01772 [hep-ex]`.

[40] CMS Collaboration. "Measurement of the $\mathrm{t\bar{t}}$ production cross section, the top quark mass, and the strong coupling constant using dilepton events in pp collisions at $\sqrt{s} = 13$ TeV". In: *Submitted to: Eur. Phys. J.* (2018). arXiv: `1812.10505 [hep-ex]`.

[41] "First combination of Tevatron and LHC measurements of the top-quark mass". In: (2014). arXiv: `1403.4427 [hep-ex]`.

[42] LHC top working group. *LHC top physics summary plots*. 2019. URL: https://twiki.cern.ch/twiki/bin/view/LHCPhysics/LHCTopWGSummaryPlots (visited on 03/03/2019).